

## Corrosion Protection of Silane Coatings Modified by Carbon Nanotubes on Stainless Steel

Ying Liu, Huaijie Cao, Yangyang Yu, Shougang Chen\*

Institute of Material Science and Engineering, Ocean University of China, Qingdao 266100, PR China.

\*E-mail: [liuyingwda@ouc.edu.cn](mailto:liuyingwda@ouc.edu.cn)

Received: 29 December 2014 / Accepted: 21 January 2015 / Published: 24 February 2015

---

The bis-[triethoxysilylpropyl] tetrasulfide (BTESPT) silane film modified by carbon nanotubes have been applied to 304 stainless steel successfully by dip-coating method. The composite coatings show better corrosion resistance property than the single silane film. The effect of multi-wall carbon nanotube (MWCNT) for the anti-corrosion properties of the BTESPT/MWCNT hybrid film is studied via electrochemical analysis technique. Scanning electronic microscopy (SEM) was performed to characterize the micro morphology. The anti-corrosion properties of the BTESPT silane film and BTESPT/MWCNT hybrid film are studied via potentiodynamic polarization tests and electrochemical impedance spectroscopy in aerating 3.5 wt% NaCl solution. The results show that the protection of BTESPT/MWCNT hybrid film is superior to silane film. At the same time, the immersion test shows that BTESPT/MWCNT silane hybrid film has a good stability in 3.5 wt% NaCl solution, so the hybrid film can prevent the penetration of the chloride ion in seawater.

---

**Keywords:** stainless steel; silane; carbon nanotubes; electrochemical impedance; corrosion resistance

### 1. INTRODUCTION

Stainless steels have been widely used in many fields, such as ships, aerospace and machinery manufacturing due to its excellent mechanical and anticorrosion performance. Despite the stainless steel is a noble metal, it will suffer corrosion when exposed to aggressive medium, such as sea water, so pretreatments for corrosion protection on stainless steel are of great importance.

Now the chromate conversion coatings are an effective pre-treatment technology for corrosion protection on metals [1, 2]. The traditional technology with good performance and low cost has been restricted due to the toxicity and carcinogenic nature of Cr<sup>6+</sup> [3]. Therefore, to develop an environmentally friendly pre-treatment method for corrosion protection on stainless steel is urgent.

Silanes as coupling agent have attracted much attention because of paint adhesion property, good corrosion inhibition and environmental friendly property [4-7]. Silane hydrolyzes when mixed into water and ethanol aqueous solution. During this process, the alkoxy groups of the silane molecules are converted into hydrophilic silanol (SiOH) groups. And these SiOH groups are easily absorbed on metal surfaces by the formation of hydrogen bonds between the SiOH groups and the surface metal hydroxyls (MOH), and the excess SiOH groups forming a siloxane network (Si-O-Si) that exhibit chemical stability and resistance to corrosive species. W.J.van Ooij[8] and Hu[9-10] had prepared the silane film on the metal surface successfully by dip-coating and electrodeposition method respectively. Some studies indicated that the silane film not only enhanced the adhesion property between the metal substrate and film, but also provided a barrier which can prevent the diffusion of corrosion ion and oxygen [11-14]. However, these films could not offer stable and long-term corrosion protection because of the presence of micropores, cracks, and areas with low cross-link density.

In addition, several works [5, 15-19] about adding nanoparticles or metal salt into the silane film for effectively reducing the defects of the silane film were reported. K.Aramaki et.al.[15] introduced cerium to the organic silane film layer to form cerium nitrate passivation film by reaction on the metal surface. Vignesh Palanivel et.al [5] investigated the protective effect of the BTESPT silane film that added SiO<sub>2</sub> nanoparticles on aluminum alloy. TiO<sub>2</sub> nanoparticles were added into silane in J.M.Hu's works [16]. These studies indicated that the corrosion protection properties had been improved significantly by introducing nanoparticles. In the composite films, the nanoparticles suffer corrosion prior, when the nanoparticles are corroded absolutely, the silane film will lose the protective properties.

Carbon nanotubes (CNTs) were applied in various fields due to their unique structural, mechanical, electronic and thermal properties [20-21]. The CNT-doped composites show favorable intensity, stress and fatigue resistance [22] and CNTs have been used as excellent hydrogen storage materials, chemical sensors and electrodes [23-24]. When used as adulterants, CNTs have been added into polyaniline coating to decrease the permeability of coating for oxygen and corrosive solution [25] and have been added into epoxy coating to increase adhesion and cohesion between coatings and metal substrates [26-27]. Although silane/CNTs composites had been studied, in their work, silane was used to modify carbon nanotubes to enhance the performance and the dispersive ability of CNTs in epoxy [28]. Introducing CNTs into silane film as the doped particles to improve the corrosion resistance of the metal substrate has rarely been studied. CNTs with long chain structures can be filled in the area of flaw and pore, delaying the crack growth in the film, so it hopefully enhances the overall compactness of the film layer.

Bis-[triethoxysilylpropyl] tetrasulfide (BTESPT) is one kind of silane that has been widely studied for corrosion protection on the metal substrate in recent years [14, 29-31]. Herein, we added dispersive CNTs into the silane solution to get the BTESPT/CNTs composite, and then the BTESPT/CNTs composite film on the 304s stainless steel surface were prepared by dip-coating method, compared with the single BTESPT film without CNTs. The electrochemical tests were performed via potentiodynamic polarization and electrochemical impedance spectroscopy (EIS) experiments were performed in 3.5 wt% NaCl solution. The evolution of the morphology and chemical composition of the films was studied using scanning electron microscopy (SEM) and energy dispersive spectrometer

(EDS). Results of electrochemical tests showed that the BTESPT/CNTs composite film has a better and more stable corrosion protection property than the single BTESPT silane film. Also different amount CNTs added into the silane film was studied in our work.

## 2. EXPERIMENTAL

### 2.1 Pre treatment for 304 stainless steel (304SS)

10 mm×10 mm×2 mm 304 SS samples were abraded with SiC sandpapers of different grade 400, 800, 1200, 2000, and then were mechanically polished 0.5 mm diamond paste. And these samples were ultrasonically cleaned with acetone, ethanol and deionized water for 10 min sequentially, respectively, and dried with N<sub>2</sub>.

### 2.2 Preparation of BTESPT/CNTs composite film

BTESPT solution was prepared by adding the BTESPT (2 vol.%) in a mixture of ethanol (95vol.%) and deionized water (3vol.%). And then the BTESPT solution was stirred for 30min, the pH of the solution was adjusted to 4.5 by adding acetic acid, and then aged at constant 25°C for 48 hours. Then 5 mg CNTs was dispersed in 10 mL ethanol by sonication for several minutes, the above-mentioned solution was doped in BTSEPT solution. The cleaned 304 SS samples were dipped into the BTESPT and the BTESPT/CNTs solutions for 30 s, and the excess solution was removed by blowing N<sub>2</sub> air (tangentially to the surface). Finally, the pre-treated samples were cured in an oven at 120°C for 1h.

### 2.3 Characterization

#### 2.3.1 Electrochemical tests

The EIS measurements and potentiodynamic polarization tests were performed with electrochemical workstation (CHI660D, CH Instruments Inc.) using a standard three-electrode cell in open-to-air 3.5 wt% NaCl solution at ambient temperature. The stainless electrode served as a working electrode, the platinum plate as a counter electrode and the saturated calomel electrode (SCE) as a reference electrode. The potential of potentiodynamic polarization was set from -600 to 600 mV at a scan rate of 2 mV/s. The EIS measurements were performed at the open circuit potential with a 10 mv amplitude sinusoidal signal and frequency ranged from 10 mHZ to 10 kHz.

#### 2.3.2 Surface morphology and composition of BTESPT/CNTs composite film

The surface morphology of the prepared samples were characterized by scanning electron microscopy (FE-SEM, JEOL-JSM-6700F) at 5.0kV. The element distributions were determined by an energy dispersive X-ray spectroscopy (EDS).

### 3. RESULTS AND DISCUSSION

#### 3.1 Effects of CNTs on the property of BTESPT/CNTs composite film

Figure 1 shows the effect of the CNTs contains corrosion resistance performance of the hybrid film. From the potentiodynamic polarization curves it can be seen that both cathode and anode corrosion current density of the BTESPT/CNTs hybrid film decreased about one order of magnitude and the corrosion potential showed more positive than that of the bare BTESPT film. This indicated that the BTESPT film doped with CNTs is more effective in improving corrosion resistance than single BTESPT film. The anodic current densities decreased because oxidation of the metal substrate and anodic reaction were suppressed, and decrease of the cathodic current densities is related to reduction of dissolved oxygen [32]. Due to existence of the doped CNTs, anodic dissolution was restrained, and the rate of charge transfer slowed down, which prevented the permeation of caustic ion effectively. Also the CNTs/silane coatings prevented excess electrons from accumulating at the metal/coating interface and the cathodic reaction was restricted. Therefore, the 304SS stainless steel coated with the BTESPT/CNTs film shows a good barrier.

In order to obtain the best corrosion resistant performance, three different proportions were selected in the experiment, 0.5 mg、2.5 mg and 5 mg contained in 10 mL silane solution respectively. From Fig.1 it can be seen that the 304ss substrate coated with the hybrid film has the better barrier property when 2.5mg CNTs were added into per 10mL silane solution. This can be explained that the CNTs change the hybrid film's chemical bonding, and affect the whole compactness of the film. When the added CNTs was excess, it could affect the condensation between the silanol, break the chemical bond and weaken the binding force of the chemical bond, which resulted in the adsorbability weakened between the film and substrate, thus reduced the barrier property of the stainless steel.

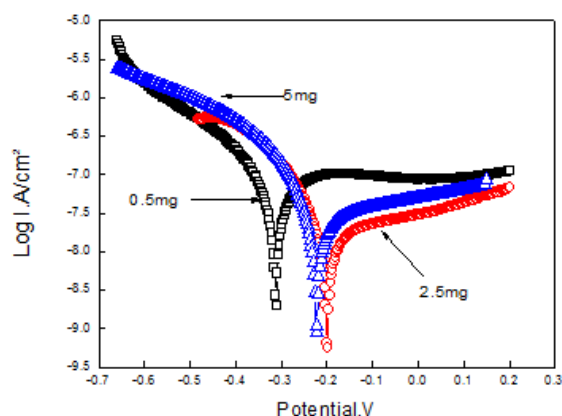


**Figure 1.** Potentiodynamic polarization curves for BTESPT/CNTs composite film with different content of CNTs.

#### 3.2 SEM characterization of surface morphology

The morphologies of the blank 304SS and sample covered with the BTESPT and the BTESPT/CNTs films are shown in Fig.2. The surface of blank 304SS (Fig.2a) is smooth, but some scratches and pits exist. The BTESPT film (Fig.2b) has a more smooth surface morphology without

any scratches as seen in others literatures [30, 33]. The microstructure of the BTESPT/CNTs composite film is presented in Fig.2c,d, which shows a dark surface with agglomeration of a number of particles.

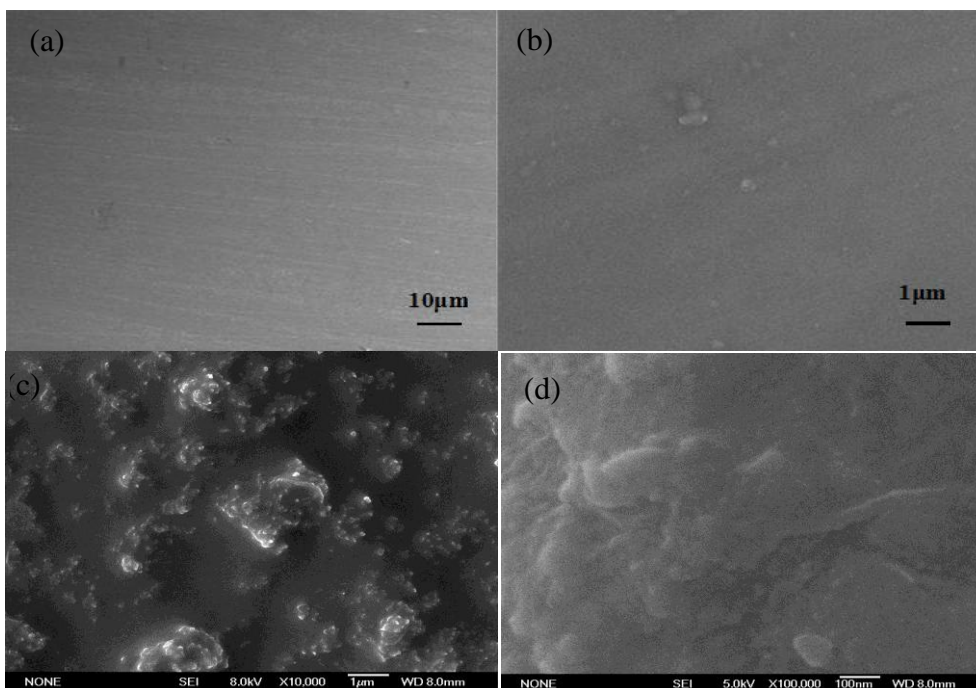


**Figure 2.** SEM images of the surface morphologies of the blank 304 SS and composite layer.(a) The blank 304 SS,(b) BTESPT,(c)-(d) BTESPT/MWCNT composite layer.

### 3.3 EDS characterization of samples for chemical composition

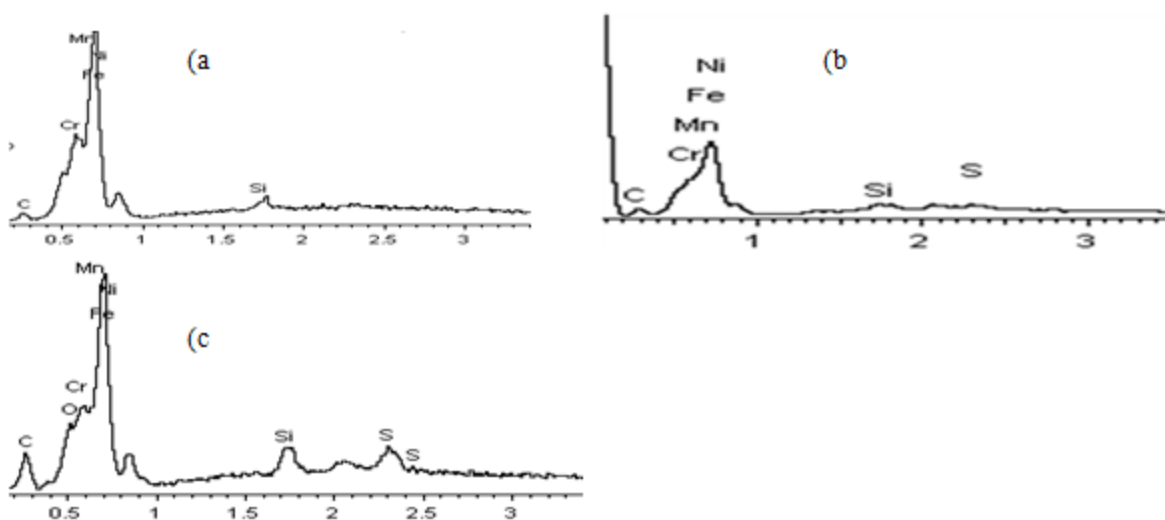


**Figure 3.** EDS spectras of the surface element of the blank 304 SS and composite layer. (a)The blank 304SS substrate,(b) BTESPT,(c) BTESPT/CNTs composite layer.

The EDS spectra on the blank 304SS and sample covered with the BTESPT and the BTESPT/CNTs films are shown in Fig. 3. Compared with the blank 304SS, the coated 304SS shows an increase in C, O and Si content. Moreover, S element appeared in the hybrid film. These results indicated that the BTESPT/CNTs films were successfully formed on the 304SS substrate

### 3.4 Potentiodynamic polarization tests of BTESPT/CNTs composite film

The potentiodynamic polarization curves of 304SS electrodes with and without film in a 3.5 wt% NaCl solution are shown in Fig.4. With the increasing of the applied voltage, the corrosion current density for the untreated 304SS electrode increased rapidly until the value of  $10^{-2}$  A/cm<sup>2</sup>. Compared with the untreated 304SS, both the cathodic and the anodic corrosion current density ( $i_{\text{corr}}$ ) of the BTESPT and the BTESPT/CNTs-coated 304SS substrates decreased obviously. The corrosion potential ( $E_{\text{corr}}$ ) shifts to the positive direction. This result suggested that the presence of the BTESPT and the composite BTESPT/CNTs films hindered anodic dissolution and retarded oxygen absorption. This restrictive effect is more obvious for the BTESPT/CNTs composite film. For the composite film, the anode current density reduced about five orders and the corrosion potential changed towards the positive direction about 0.4 V. This indicated that the BTESPT film doped with CNTs is more effective in improving corrosion resistance than single BTESPT film, which is because of the formation of the M-O-Si covalent bonds at the interface, so the BTESPT film and the stainless steel substrate were combined tightly by the chemical bond [34-36]. Also the CNTs can enhance the compactness of the film and substrate, hinder the permeation of corrosive medium ions effectively, and restrain the diffusion of corrosion products. The result shows that the BTESPT/CNTs composite film can effectively protect the substrate from corrosion.

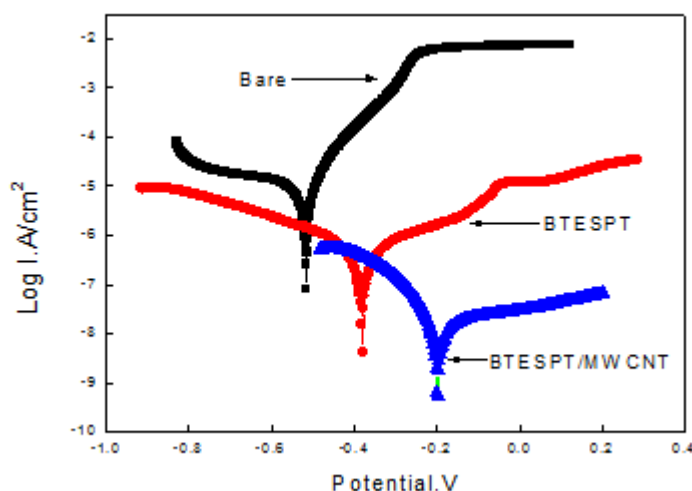


**Figure 4.** Potentiodynamic polarization curves of stainless steel blank sample and composite films

The thermodynamic and kinetic parameters of electrochemical corrosion were obtained by extrapolation from the polarization curves. These parameters included the open circuit potential

(OCP), anodic and cathodic Tafel slopes ( $\beta_a$ ,  $\beta_c$ ), corrosion potential ( $E_{corr}$ ), corrosion current density ( $i_{corr}$ ), polarization resistance ( $R_p$ ) and inhibition efficiency ( $\eta_P$ ), which are summarized in Table 1. The inhibition efficiency ( $\eta_P$ ) was calculated by the following equation 1 [37],

$$\eta_P \% = \frac{(i_{corr}^0 - i_{corr})}{i_{corr}^0} \times 100 \quad (1)$$

As shown in Table 1, the existence of the films reduces both the anodic and cathodic currents, and there is a significant positive shift for the corrosion potential. Thus, the coverage of the films reduced the corrosion rate of the 304 SS, especially for the substrate with BTESPT/CNTs composite film. The  $\eta_P$  values of the BTESPT/CNTs film can reach 99.3. And corrosion current density ( $I_{corr}$ ) of BTESPT/MWCNT film can reach  $4.374 \times 10^{-3} \mu\text{A} \cdot \text{cm}^{-2}$ , which is lower than that of cerium doped silica sol-gel coatings system for corrosion protection on stainless steel [38].

**Table 1.** The polarization parameter of stainless steel blank sample and composite films in 3.5 wt.% NaCl solution

sample	Ocp (V)	$B_a$ (mV·dec <sup>-1</sup> )	$B_c$ (mV·dec <sup>-1</sup> )	$E_{corr}$ (V)	$I_{corr}$ ( $\mu\text{A} \cdot \text{cm}^{-2}$ )	$R_p$ (k $\Omega \cdot \text{cm}^2$ )	$\eta_P$ (%)
304SS	-0.529	59.5	49.1	-0.517	0.4116	2.837	—
BTESPT	-0.289	58.6	35.5	-0.363	$1.701 \times 10^{-2}$	1086	95.8
BTESPT/MWCNT	-0.139	110.1	454.7	-0.2269	$4.374 \times 10^{-3}$	1120	99.3

### 3.5 EIS tests of different samples

The EIS results of the 304SS substrates coated by BTESPT with and without CNTs after 30 minutes immersion in 3.5 wt% NaCl solution are presented in Fig.5. The reference curves for the bare 304SS are similarly presented in the same figure. Fig.5 (a) is Nyquist diagram of stainless steel substrate with and without film, the Impedance arc radius is larger, the protecting effect is better. The impedance arc of treated 304SS is larger than the bare 304SS, and the impedance arc of hybrid film increases obviously compared with the single BTESPT film.

In bode plot, the impedance at high frequency corresponds to the property of the film, concerned with the compactness and hydrophobic property of the film, while the impedance modulus at low frequency is related to the corrosion resistance [39, 40]. High impedance in sample is ascribed to an area effect where the coating is blocking the aggressive electrolyte from reaching the reactive metal surface. The impedance modulus at low frequency is larger, the corrosion resistance property is better. From Fig.5 (b) it can be seen that the impedance modulus of hybrid film is larger than the impedance of bare 304ss and BTESPT film. The impedance modulus of the hybrid film has reached about  $10^{7.3} \Omega \text{cm}^2$ , which is three orders of magnitude larger than the bare 304SS and two orders of magnitude higher than the pure BTESPT film. The blue curves in Fig.5 demonstrated an enhancement

in the barrier properties of the hybrid coatings in the presence of CNTs. Compared with other doped silane coatings, the impedance modulus of the BTESPT/CNTs hybrid film is higher than that of cerium doped silica sol-gel coatings [38] system and nanoclay incorporated silane coating system [41]. These results suggested that CNTs are important for the corrosion protection of the BTESPT/CNTs composite film.

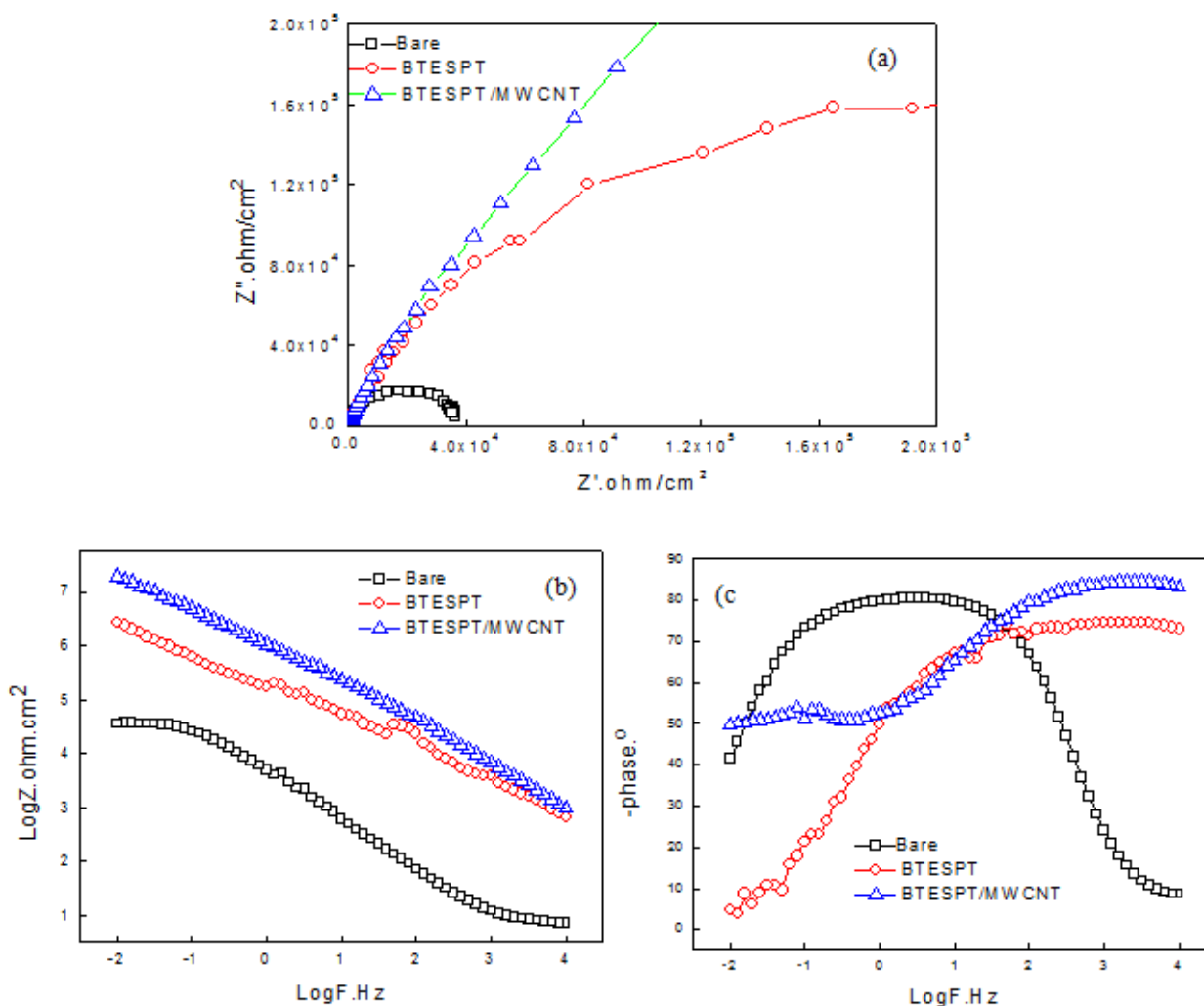


**Figure 5.** (a) Nyquist curve (b) Bode curve (c) Phase angle figure of stainless steel blank sample and stainless steel after modification.

The phase angle diagram Fig.5(c) shows the differences among the curves of the three substrates. The curve of the bare 304 SS displays only one wide platform at medium frequency zone. By contrast, the wide platform appeared in the regions of high to medium frequency zone in the curves of the coated samples. The phase diagram is used to characterize the capacitance and impedance performance of the layer. The higher the phase angle, the greater of capacitive character of the membrane layer, and the stronger of the inhibition of the permeability of corrosion medium, as reported elsewhere [30, 42-43]. From Figure5(c), it can be seen that the phase angle of the coated



stainless steel sample increased obviously, especially for the BTESPT/CNTs composite film, the phase angle close to ninety degrees, which shows excellent corrosion resistance performance. This can be explained that the BTESPT/CNTs composite film has better corrosion resistance performance than the BTESPT film. So the results are consistent with the analysis of the Nyquist diagram and bode plot.

In order to analysis these results, equivalent circuit model was used to simulate the electrochemical impedance data, and calculate the protection efficiency of different membrane layer on the stainless steel substrate. The protection efficiency ( $\eta_E$ ) of films can be determined from Eq.2 [44]:

$$\eta_E \% = \frac{(R_t - R_t^0)}{R_t} \times 100 \tag{2}$$

In this circuit, as shown in Figure 6,  $R_t$  is the charge transfer resistance,  $Q_t$  is the constant phase element of the electrical double layer,  $R_s$  is the solution resistance,  $Q_f$  and  $R_f$  represent the capacitance and resistance of the composite coatings. BTESPT/CNTs composite film are fit with R(Q[R(QR)]) circuit. Compared with BTESPT film, lower value of  $Q_f$  was observed for BTESPT/CNTs composite film from Table 2. So the added CNTs had a beneficial impact on the coating capacitance and improve the corrosion protection of BTESPT film.

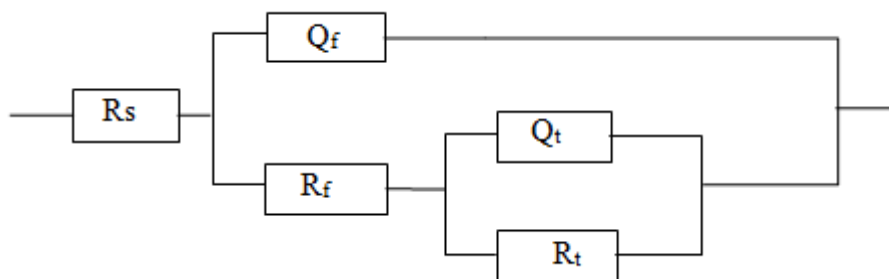


**Figure 6.** Equivalent circuits for 304SS coated with composite film.

**Table 2.** Electrochemical impedance parameters for the composite film-coated stainless steel and the bare stainless steel in 3.5 wt% NaCl solution at room temperature

Samples	$R_s$ ( $\Omega \text{ cm}^2$ )	$R_f$ ( $\text{k}\Omega \text{ cm}^2$ )	$Q_f$ ( $\mu\text{F cm}^{-2}$ )	$n_{Qf}$	$Q_t$ ( $\mu\text{F cm}^{-2}$ )	$n_{Qt}$	$R_t$ ( $\text{k}\Omega \text{ cm}^2$ )	$\eta_E$ (%)
304SS	11.2	—	—	—	69.9	0.902	164	—
BTESPT	81.8	135	4.32	0.700	3.63	0.787	1010	83.7
BTESPT/ MWCNT	131	220	0.0837	0.854	0.205	0.585	2100	96.6

### 3.6 Corrosion resistance of the sialne films

The long-term environmental stability of protective films is significant for practical applications. Thus, the durability of the BTESPT and the BTESPT/CNTs films were evaluated in 3.5 wt% NaCl solution.

When the BTESPT-treated substrates were immersed in the 3.5 wt% NaCl solution, a pronounced drop in the low-frequency impedance region was observed from around  $10^{6.5} \Omega \text{ cm}^2$  to  $10^5$

$\Omega \text{ cm}^2$  with the prolongation of immersion time (Fig. 6a). At the end of the tests, the BTESPT films almost lost protective property because of the heavily localized corrosion caused by the penetration of the electrolyte, and similar results had also been found in other literatures [33, 38]. For the systems treated with CNTs-modified BTESPT, the impedance value at low frequency region is still high after immersion for 30 days. It shows that the significant improving in corrosion resistance of composite films can be attributed to the addition of CNTs. The added CNTs can change the internal structure of the films, increase the density of the membrane layer.

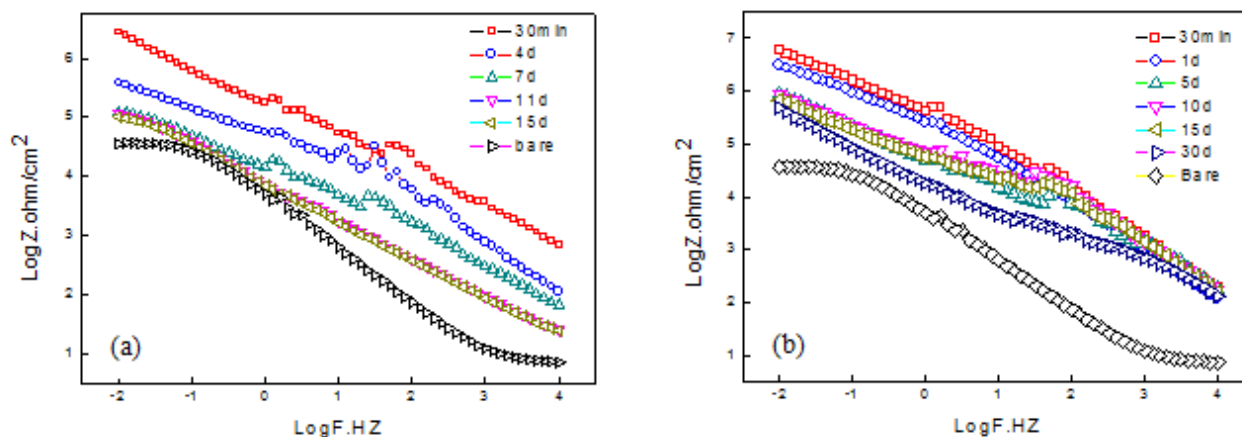


**Figure 7.** The Bode plots of films after immersion different period (a) BTESPT film, (b) BTESPT/MWCNT film.

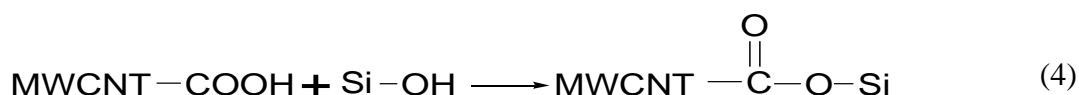
### 3.7 Mechanism of corrosion protection of BTESPT/CNTs composite films

When silane is hydrolyzed in an aqueous environment, the alkoxy groups of the silane molecules are converted into hydrophilic silanol (SiOH) groups. These SiOH groups are easily absorbed by metal surfaces via the formation of hydrogen bonds between the SiOH groups and the surface metal hydroxyls (MOH). By producing water, these weak bonds are further converted into metallo-siloxane bonds (MOSi) at the interface. In high temperature, condensation likewise occurs among the excess SiOH groups to form a siloxane network [45] (Si-O-Si) that exhibits chemical stability and resistance to corrosive medium [46].

The following reactions for hydrolysis and condensation of silanes (e.g., BTESPT) during the formation of films have been proposed.



Because of the existence of the single BTESPT film structural defects, such as porous and fissure, the protective effect of the single silane film on metal is not good. Once the coating has been damaged, the film would lose the protective effect. In this experiment, the used CNTs is carboxylation MWCNTs. When the moderate carbon nanotubes were added into the hydrolysis of silane solution, they could react with the silane hydrolyzate Si (OH), and the equation is as follows:



The chemical bond between MWCNT and silane can strengthen the adhesion strength of the film, increase the density of the composite film and inhibit the pervasion of the corrosive ions. In addition, due to the long chain structure, the carbon nanotubes may fill the pit and crack in the film, delay the extension of crack effectively, and make the film become denser. So it enhances the corrosion resistance of matrix effectively.

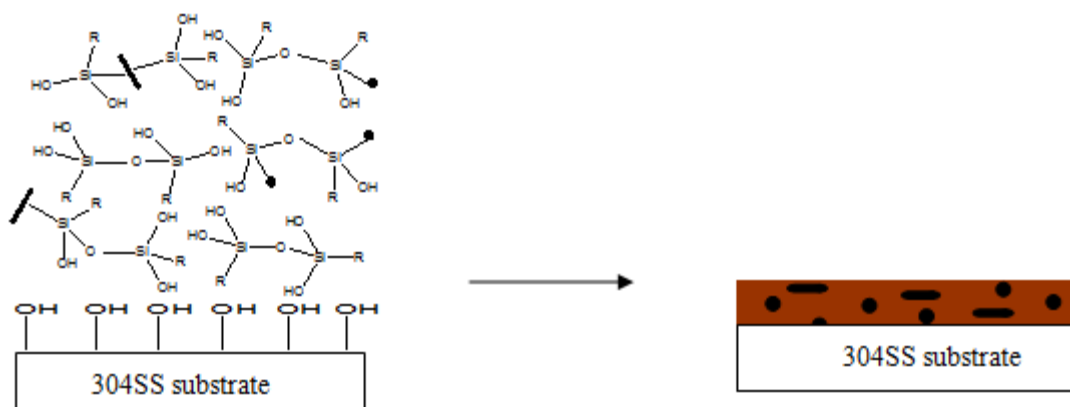


**Figure .8** Mechanism of corrosion protection of BTESPT/CNTs composite films.

#### 4. CONCLUSIONS

BTESPT film and BTESPT/CNTs composite film were prepared on 304SS successfully by dip coating method in this study. From the electrochemical results, both the BTESPT film and BTESPT/CNTs composite film showed corrosion protection for the stainless substrates. But the BTESPT modified by the doped CNTs had better corrosion resistance than the single BTESPT film. Due to the doped CNTs, the composite films were more densified, which contributed to the improvement of the corrosion protection of the composite film.

#### ACKNOWLEDGEMENTS

This study was supported by the National Nature Science Foundation of China (NSFC, 21203171).

#### Reference

1. A. Conde, M. A. Arenas, A. de Frutos and J. de Damborenea, *Electrochim. Acta*, 53(2008) 7760
2. L. M. Palomino, P. H. Suegama, I. V. Aoki, M. F. Montemor and H.G. De Melo, *Corros. Sci.* 120(2009) 236
3. W. Trabelsi, L. Dhouibia, E. Triki, M. G. S. Ferreira and M.F. Montemor, *Surf. Coat. Technol.* 192 (2005) 284
4. W. J. van Ooij. In the SIP seminar on Chromate Replacements, Oslo, Norway, March 18-19, 2002

5. D. Zhu and W. J. van Ooij, *Prog. Org. Coat.* 49(2004)42
6. V. Subramanian and W. J. van Ooij, *Surface Engineering*, 15(1999)1
7. T. F. Child and W. J. van Ooij, *Trans IMF*, 77(1999)64-70
8. W. J. van Ooij. In the SIP seminar on Chromate Replacements, Oslo, Norway, March 18-19, 2002
9. J. M. Hu, L. Liu, J. Q. Zhang and C.N. Cao, *Electrochim. Acta*, 51(2006)3944
10. L. K. Wu, J. T. Zhang, J. M. Hu and J. Q. Zhang, *Corros Sci.* 56(2012) 58
11. A. M. Cabral and R.G. Duarte, *Prog. Org. Coat.* 54(2005)322
12. B. Chico and J. C. Galvan, *Prog. Org. Coat.* 60(2007)45
13. M. F. Montemor, A. Rosqvist, H. Fagerholm and M. G. S. Ferreira. *Prog. Org. Coat.* 51(2004) 188
14. M. A. Chen, N. Cheng, J. M. Li and S. Y. Liu, *Surface Engineering*, 28 (2012) 491
15. K. Aramaki. *Corros.Sci.* 47(2005)1285
16. J. M. Hu, L. Liu, J. Q. Zhang and C. N. Cao, *Electrochim. Acta*, 51(2006)3944
17. R. Zandi Zand, K. Verbeken, A. Adriaens, *Int. J. Electrochem. Sci.*, 8 (2013) 4924
18. S. L. Zhang, M. M. Zhang, Y. Yao and F. Sun, *Transactions of the Institute of Metal Finishing*, 89 (2011) 320
19. M. J. Palimi, M. Rostami, M. Mahdavian and B. Ramezanzadeh, *J Sol-Gel Sci Technol.* 73 (2015) 141
20. S. C. Canobre, D. A. L. Almeida, C. P. Fonseca and S. Neves, *Electrochim Acta*, 54(2009)6383
21. W. Jarernboon, S. Pimanpang, S. Maensiri, E. Swatsitang and V. Amornkitbamrung, *J. Alloys Comp.* 476(2009)840
22. S. H. S. Zein, L. C. Yeoh, S. P. Chai, A.R. Mohamed and M.E.M. Mahayuddin, *J. Mater. Proc. Technol.* 190 (2007) 402
23. A. C. Dillon, K.M. Jones, T.A. Bekkedahl, C.H. Kiang, D.S. Bethune and M.J. Heben, *Nature*, 386 (1997) 377
24. P. Serp, M. Corrias and P. Kalck, *Appl.Catal. A*, 253 (2003) 337
25. M. A. Deyab, *Journal of Power Sources* 268 (2014) 50
26. S. Ganguli, H. Aglan, P. Dennig, *J. Reinf, Plast. Compos.* 25 (2006) 175
27. H. R. Jeon, J.H. Park, M.Y. Shon, *J. Ind. Eng. Chem.* 19 (2013) 849
28. P. C. Ma, J. K. Kim and B. Z. Tang, *Composites Science and Technology* 67 (2007) 2965
29. F. Zucchi, A. Frignani, V. Grassi, A. Balbo and G. TrabANELLI. *Mater. Chem. Phys.* 110(2008)263
30. W. Xiao, R. Man, C. Miao and T. L. Peng, *Journal of Rare Earths*, 28 (2010) 117
31. L. K. Wu, L. Liu, J. Li, J. M. Hu, J. Q. Zhang and C. N. Cao, *Surf. Coat. Technol.* 204 (2010) 3920
32. P. Balan, M. J. Shelton, D. O. Li Ching, G. C. Han and L. K. Palniandy, *Procedia Materials Science* 6 ( 2014 ) 244
33. M. A. Chen, R. Huang and X. B. Lu, *Corrosion Engineering, Science and Technology* 46 (2011) 712
34. M. Honkanena, M. Hoikkanen, M. Vippola, J. Vuorinen, T. Lepistö, P. Jussila, H. Ali-Löytty, M. Lampimäki and M. Valden, *Applied Surface Science* 257 (2011) 9335
35. S. M. Hanetho, I. Kaus, A. Bouzga, C. Simon, T. Grande and M.-A. Einarsrud, *Surf. Coat. Technol.* 238 (2014) 1
36. D. Balgude and A. Sabnis, *J Sol-Gel Sci Technol* 64 (2012) 124
37. X. P. Ouyang, X. Q. Qiu, H. M. Lou, D. J. Yang, *Ind. Eng. Res.* 45 (2006) 5716
38. R. Zandi Zand, K. Verbeken, A. Adriaens, *Prog. Org. Coat.* 75 (2012) 463
39. N. Asadi, R. Naderi and M. Saremi, *Appl. Clay Sci.* 95 (2014) 243
40. N. Asadi, R. Naderi, M. Saremi, S. Y. Arman, M. Fedel and F. Deflorian, *J. Sol-Gel Sci. Technol.* 70 (2014) 329
41. F. Ansari, R. Naderi and C. Dehghanian, *RSC Adv.* 5 (2015) 706
42. L. E. M. Palomino, P. H. Suegama, I. V. Aoki, Z. Paszti, H. G. de Melo, *Electrochim. Acta* 52 (2007) 7496

43. R. Zandi Zand, V. Flexer, M. D. Keersmaecker, K. Verbeken, A. Adriaens, *Int. J. Electrochem. Sci.*, 10 (2015) 997
44. S. L. Li, Y. G. Wang, S. H. Chen, R. Yu, S. B. Lei, H. Y. Ma, D. X. Liu, *Corros. Sci.* 41 (1999) 1769
45. V. Palanivel, D. Q. Zhu and W. J. van Ooij. *Prog. Org. Coat.* 47 (2003) 384
46. A. Cabral, R. G. Duarte, M. F. Montemor, M. L. Zheludkevich and M. G. S. Ferreira, *Corros. Sci.* 47 (2005) 869

© 2015 The Authors. Published by ESG ([www.electrochemsci.org](http://www.electrochemsci.org)). This article is an open access article distributed under the terms and conditions of the Creative Commons Attribution license (<http://creativecommons.org/licenses/by/4.0/>).